Wide-angle seismic profiling of arc-arc collision zone in the northern Izu-Ogasawara arc – KY0408 cruise –

Narumi Takahashi*, Shuichi Kodaira*, Takeshi Sato*, Aki Ito*, Tetsuo No* and Yoshiyuki Kaneda*

Abstract We carried out a deep wide-angle seismic experiment using a large airgun array and total 103 ocean bottom seismographs (OBSs) in the northern Izu-Ogasawara arc area, which was conducted by R/V Kaiyo of Japan Agency for Marine-Earth Science and Technology (JAMSTEC) from July 8, 2004 to July 22 (KY04-08 cruise). Objectives of this cruise are to know a velocity structure of the arc-arc collision zone and to understand relationship between the crustal growth and the arc collision, which is one of important parameters to clarify nature of the oceanic arc growth. An airgun-OBS seismic line was set from western Sagami Bay near granitic Izu peninsula to Tori-shima along the direction of the volcanic front. We shot a large airgun array with total volume 12,000 cu. in. and recorded the seismic signals on OBSs with four components and a hydrophone streamer. In this paper, we summarize information of the seismic experiments and introduce OBS data and reflection data.

Keywords: Crustal structure, seismic, wide-angle data, OBS, Izu-Ogasawara, granitic layer

1. Introduction

An oceanic island arc is one of the best examples to study a process of crustal growth, because the crustal growth had been started by a subduction of an oceanic crust beneath the other oceanic crust and because the tectonic history is simpler than that of a continental arc, which had been separated from the continental margin with complex structure. An oceanic arc crust is constructed by 'a subduction factory' (e.g., Tatsumi, 2002), however, it is said that it is difficult to make a continental crust only by subduction (Taira et al., 1997). It is thought that the arc-arc collision is one of the important elements to construct granitic middle crust, whose process is however, still poorly understood.

The Izu-Ogasawara arc has granitic middle crust with P-wave velocity (Vp) of 6 km/s and relatively thick lower crust (e.g., Suyehiro et al., 1996). And the crust of the northern Izu-Ogasawara arc is regarded as a matured island arc crust. The crustal growth has been started by a subduction between two oceanic plates located western old Pacific since Eocene time (e.g., Karig and Moore, 1975), and it is said that the initial oceanic arc did not have the granitic layer (e.g., Tatsumi et al., 2004). Macpherson and Hall (2001) suggested that there was initial plume activity with basalt-type magmatism and that the granitic crust has been generated at almost same time with high heat flow. This story is a little different with that of Karig and Moore (1975), however, it is common that there was no granitic layer in the initial stage of arc generation. After the Shikoku and the Parece Vela basins spread during about 30-15 Ma (e.g., Okino et al., 1998), newly volcanism had started near current position of the arc and the oceanic arc has been growing. We believe that these crustal structures have information related such crustal growth history.

To understand above crustal growth history, we focus the crustal growth by arc-arc collision and image crustal thickening and shortening. A basement high called the Shinkurose in the northern Izu-Ogasawara arc had been developed by the crustal thickening (Aoike et al., 2001). A wide-angle refraction study (Nakanishi et al., 1998), a reflection study (Takahashi et al., 2002) and a microseismicity study (Shiobara et al., 1996) ahve revealed that the initiation of new subduction at southern foot of the Zenisu ridge has been occurred by. The crustal shortening should be possible on the northern part of this arc extended from the southern foot of the Zenisu ridge.

Recently, the hot finger hypothesis was proposed by Tamura et al. (2002). It is said that the "hot finger" exists in upper mantle and causes the spatial heterogeneity of the volcanoes along the arc. If there are such variations of the upper mantle, the degree of the crustal differentiation might be also difference between the hot and the cold areas.

The objectives of this cruise are to image above crustal thickening and shortening by arc-arc collision and the heterogeneous structure along the arc, and understand natures of the crustal growth and differentiation not only by a subduction factory but also by an arc-arc collision.

* Japan Agency for Earth-Marine Science and Technology

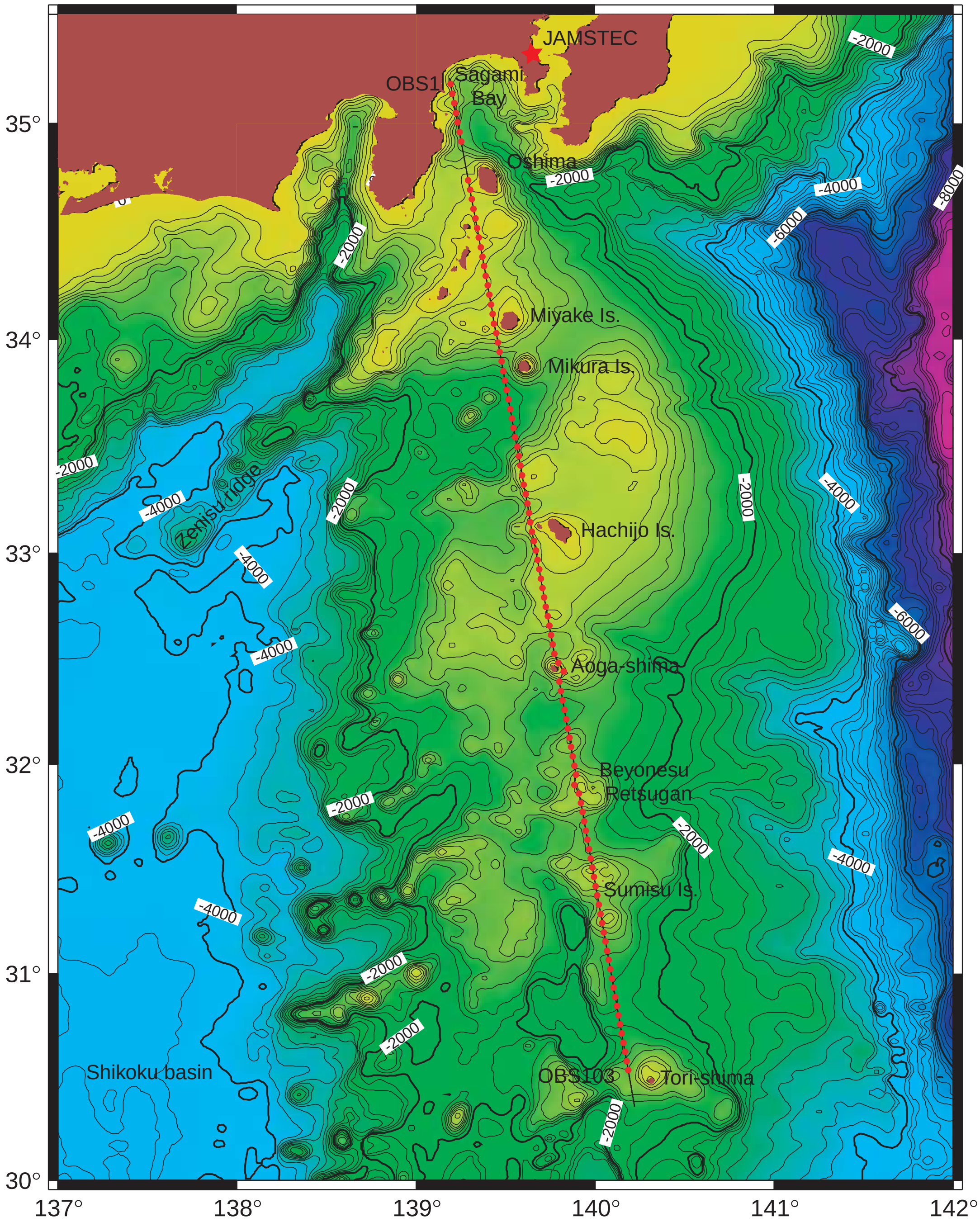

Figure 1: Map of the experimental area. Solid circles indicate OBSs. We shot an airgun array on a thick black line.

2. Experiment

We carried out a wide-angle seismic survey using an airgun array and ocean bottom seismographs (OBSs) to achieve above objectives (Figure 1). This cruise using R/V "Kaiyo" of Japan Agency for Marine-Earth Science and Technology (JAMSTEC) consists of two legs; first leg is from July 8 to July 20 and second leg is from July 20 to July 27. The R/V Kaiyo departed from JAMSTEC (Yokosuka) at July 8 and started OBS deployment from the northern part until July 11. Then airgun shooting was carried out until July 14 in northern half of the line. Then, we recovered 27 OBSs deployed in northern part during July 15 to 17. After that, we deployed OBSs again in the southern part until July 18. Airgun shooting was carried out until July 20, and then we stopped at Port Sokodo, Hachijo Island to change researchers. On the same day, The R/V Kaiyo departed there and we started airgun shooting again from July 21 to 24. Then we recovered 76 OBSs until July 27 and arrived at JAMSTEC at July 28. The actual activities are shown in Table 1 and Figure 2.

To clarify heterogeneous structure by arc-arc colli-

Table 1: Activity log during KY0408 cruise.

Date	Remarks
July 08	Departure from JAMSTEC, staring OBS deployment (OBS#1-OBS#18)
July 09	OBS deployment (OBS#19-OBS#60)
July 10	KY0408-1 airgun shooting
July 11	KY0408-1 airgun shooting and stopping shooting for emergency retrieval of OBS21
July 12	OBS21 retrieval
July 13	OBS21 deployment again and re-starting KY0408-1 airgun shooting
July 14	KY0408-2 airgun shooting
July 15	Finish of KY0408-2 airgun shooting and starting OBS retrieval (OBS#27-OBS#21)
July 16	OBS retrieval (OBS#1-OBS#17)
July 17	OBS retrieval (OBS#18-OBS#23) and OBSdeployment (OBS#61-OBS#79)
July 18	Finish of OBS deployment (OBS#80-OBS#103) and starting KY0408-3 airgun shooting
July 19	KY0408-3 airgun shooting
July 20	KY0408-3 airgun shooting and , stopped at Hachijo Is.
July 21	Re-starting KY0408-3 airgun shooting and KY0408-4 airgun shooting
July 22	KY0408-4 airgun shooting
July 23	KY0408-4 airgun shooting
July 24	Finish of KY0408-4 airgun shooting and starting OBS retrieval (OBS#103-OBS#91)
July 25	OBS retrieval (OBS#90-OBS#67)
July 26	OBS retrieval (OBS#66-OBS#43)
July 27	OBS retrieval (OBS#42-OBS#28)
July 28	Transit and arrival at JAMSTEC

sion and characteristics of matured oceanic arc, we need a long line to cover the whole collision zone. Seismic line was settled as the following requirements are satisfied: (1) to locate near the Izu Peninsula with the granitic block, (2) the position of the seismic line to be basement highs within the rifted zone, because characteristics of the seismic structure are different between the rifted zone and the forearc region, (3) to avoid small basins in the rift area near the Hachijo Island, the Sumisu Island and Tori-shima, because crustal deformation with low velocity block should be by rifted activity with a lot of normal faults, and (4) to take tie with previous seismic lines by Suyehiro et al (1996) and Nishizawa et al (2003) to keep the reliability. Considering the above issues, we set the main line with the length of about 540 km from the Sagami Bay to the Tori-shima. The line runs through the western side of the volcanic front and avoids the depression areas within the rifted zone. The northern and southern ends of the main line are (35°10'57.49"N, 139°11'31.98"E) and (30°26’2.81”N, 140°12’19.05”E), respectively. If the line locates on or nearby islands, we moved the line about two miles from coastline for safety (Figure 1).

One of typical structural characteristics of arc-arc collision might be expressed as a variety of crustal thickness and heterogeneousness along the arc. To detect deep seismic structure to the upper mantle, a length of the seismic line should be longer than a few hundred kilometers and airgun signals from long offset should be recorded on each OBS. To detect heterogeneity of the crust by past tectonics and the distribution of volcanoes, the obtained structure should have high resolution less than 10 km for deeper part. Therefore, we deployed 103 OBSs with an interval of 5 km and an airgun array with 12,000 cubic inches capacity as the source to realize the above requests. This area has complicated sedimentary structure relating to distribution of volcanoes. We recorded airgun signals by not only OBSs but also a 12-channel hydrophone streamer to know nature of the shallow structure.

2.1 Airgun shooting

Due to high topographic variation, expected S/N ratio of a part of the OBS records are low. To keep good quality of the OBS data, we took duplicated high spatial shooting with 100 m interval (about 70-100 sec interval depending on the ship speed). Because the length of the seismic line is relatively long, we separated the line into two parts (northern and southern part) to reduce risk against bad weather and severe sea statement by typhoons and low pressures (Figure 3). The northern part is from northern end of the line to Aoga-shima (Lines ky0408-1 and ky0408-2) and southern is from Mikura Island to Tori-shima (Lines ky0408-3 and ky0408-4). Table 2 shows the shooting log.

The airgun array with total capacity of 12,000 cubic inches consists of eight Bolt Longlife Airguns with 1,500 cubic inches capacity each. The air pressure sent to the chamber was 2,000 psi. The geometry of the seismic experiment is shown in Figure 4. The two floats

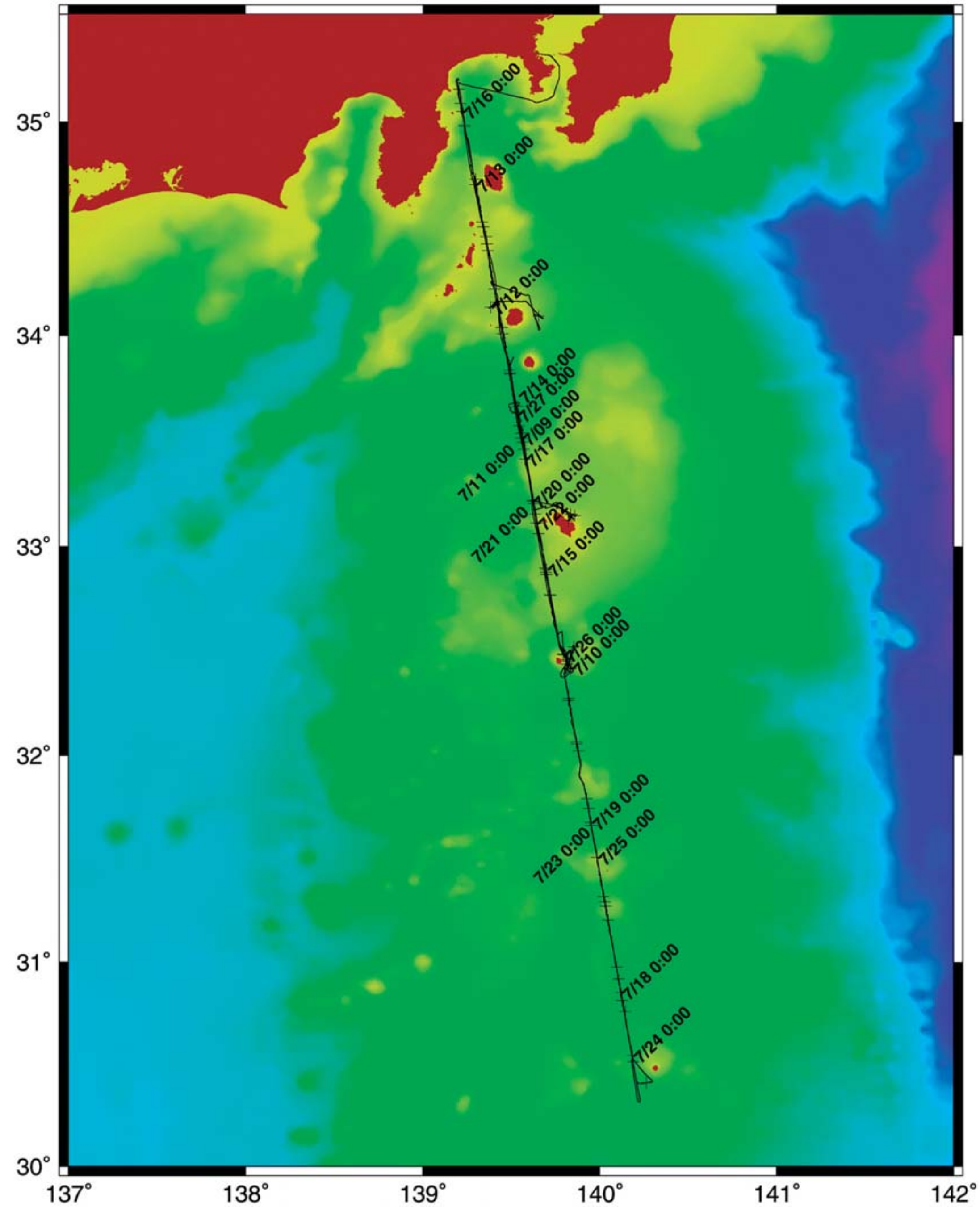

Figure 2: Map for ship's track line. Cross marks indicates ship position of every 6 hours.

with two airguns each were deployed from port and starboard sides, respectively. The airgun array's size is 34.56 m length x 21.3 m width. Airgun's position was kept 148.2 m behind the ship position (distances from ship antenna to the stern, and from the stern to center of the airgun array, are 30 m and 110.2 m, respectively).

As the differential global positioning system (DGPS) of the ship navigation system, Skyfix system was used (Sapporo as the nearest station). However, because we have experienced the emergency stop of airgun shooting due to non-succession of GPS data in the past, we introduced StarFire system for seismic navigation system in this cruise. Ship navigation system by Skyfix was used as backup of the seismic navigation system. The accuracy of shooting position was about 10 m.

2.2 Ocean Bottom Seismographs

We deployed 103 OBSs on the seismic line (Figure 1, Table 3). The interval of each OBS is 5 km and was decided by 2-D ray tracing using expected velocity model referring to that of Izu-Ogasawara arc (Suyehiro et al., 1996; Takahashi et al., 1998). However, because

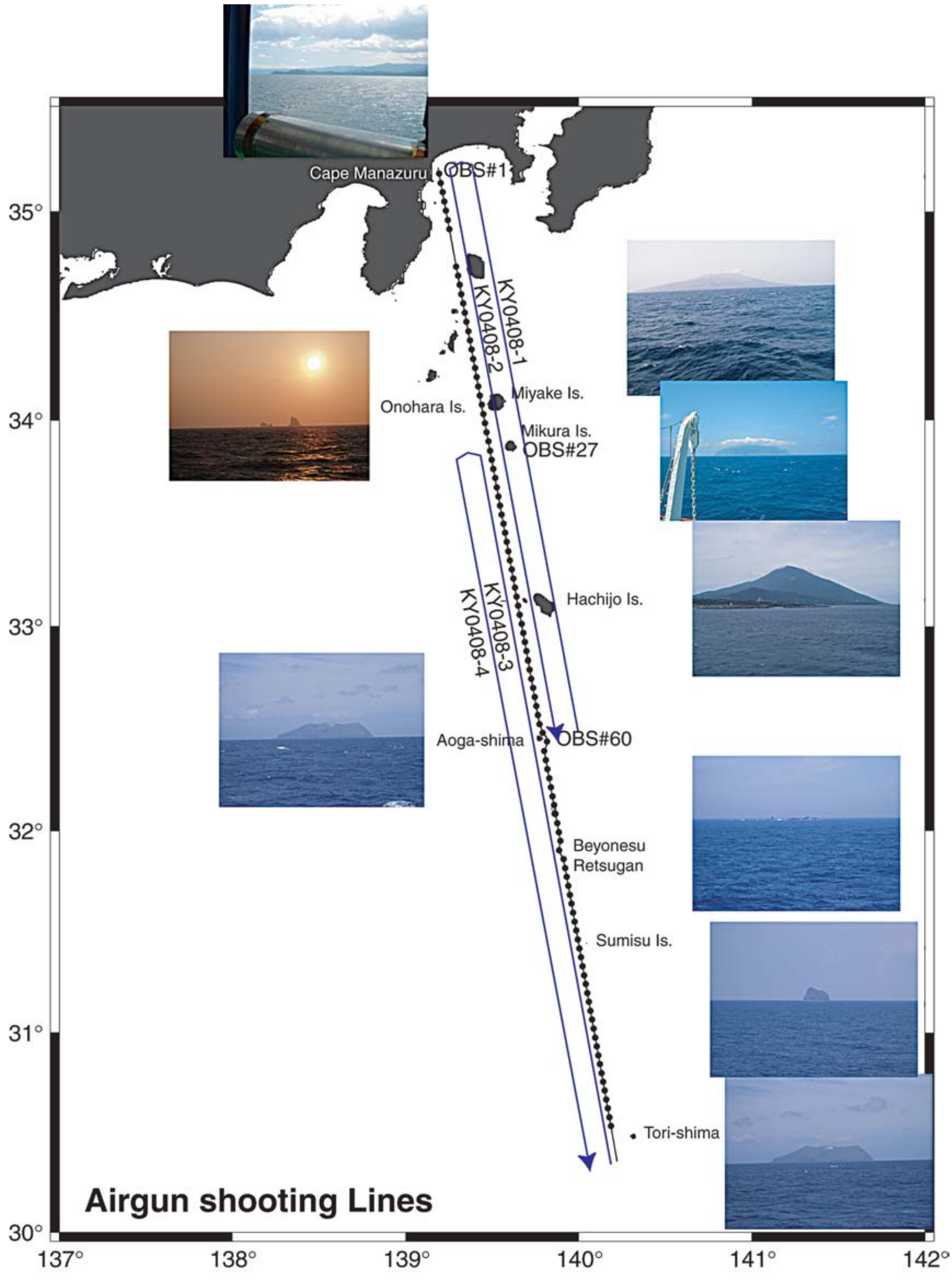

Figure 3: Map of airgun shooting. Blue arrows show a direction of the shooting.

there is a regular course of general ships between the Oshima and the Sagami Bay, we did not deploy OBSs in the area. All OBSs were recovered, however, five OBSs has no data due to troubles of recording system.

All OBSs were equipped with three-component geophones (vertical and two horizontal components perpendicular each other) using gimbal-leveling mechanisms and a hydrophone sensor. Natural frequency of these geophones was 4.5 Hz. The sensitivities of a geophone and hydrophone sensors are shown in Table 4. Our OBSs and the digital recorder system were originally designed by Kanazawa and Shiobara (1994) and Shinohara et al. (1993) as shown in Figure 5. The digital recorder used a 16-bit A/D converter and stored data on

Table 2: Airgun shooting log.

KY0408-1	Time (UTC)	Latitude (N)	Longitude (E)	Depth(m)	SP
First shot	2004.7.11 7:07	32° 26.9835'	139° 49.2772'	531	1005
Stop shot	2004.7.12 11:59	34° 12.9647'	139° 24.4757'	438	2006
Restart shot	2004.7.13 2:03	34° 11.2585'	139° 24.8345'	434	1990
Last shot	2004.7.13 14:51	35° 10.9582'	139° 11.5330'	775	2551

KY0408-2	Time (UTC)	Latitude (N)	Longitude (E)	Depth(m)	SP
First shot	2004.7.13 15:24	35° 11.0153'	139° 11.5403'	820	1001
Stop shot	2004.7.14 17:58	33° 34.7277'	139° 32.8533'	1629	1906
Restart shot	2004.7.15 0:16	33° 38.9915'	139° 31.9193'	1618	1866
Last shot	2004.7.15 17:31	32° 26.6372'	139° 49.4603'	499	2551

KY0408-3	Time (UTC)	Latitude (N)	Longitude (E)	Depth(m)	SP
First shot	2004.7.19 7:04	30° 26.0468'	140° 12.3175'	1160	995
Stop shot	2004.7.19 22:32	33° 11.6065'	139° 37.8302'	872	2559
Restart shot	2004.7.20 23:45	33° 11.2860'	139° 37.8940'	858	2556
Last shot	2004.7.20 10:59	33° 51.4243'	139° 29.2403'	1415	2933

KY0408-4	Time (UTC)	Latitude (N)	Longitude (E)	Depth(m)	SP
First shot	2004.7.20 11:34	33° 51.9748'	139° 29.0687'	1409	1744
Stop shot	2004.7.21 0:36	33° 26.8860'	139° 39.2947'	537	2191
Restart shot	2004.7.21 2:48	33° 63.7060'	139° 39.2225'	493	2191
Last shot	2004.7.22 20:44	30° 54.2260'	140° 13.7095'	1545	3748

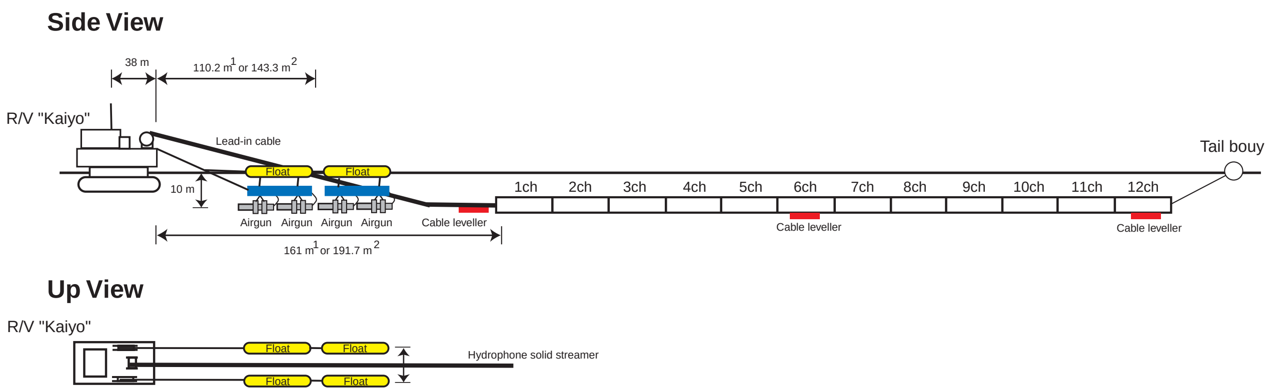

Figure 4: Geometry of airgun system and the hydrophone streamer.

digital audiotape or a hard disk sampling continuously with original format (Shinohara et al., 1993). The electronic power for the recorder system of OBS is supplied by rechargeable lithium-ion or alkali batteries. Above geophone sensors with gimbal-leveling mechanism, batteries and a recorder system are installed in 15 inch glass sphere by Benthos, Inc. The glass sphere is stored in the yellow hard hat. To enable easy OBS retrieval after arriving at sea surface, each OBS is attached to a flash light and a beacon with coded signals.

An OBS is deployed by free fall and retrieved by melting releaser composed of stainless steel plates connecting the OBS with a weight when a transponder system receives acoustic signal sent from a vessel. This acoustic communication between the OBS and the vessel was performed using transducers installed on the vessel. Positions of OBSs on sea bottom are estimated by SSBL of the vessel's positioning system during the cruise.

After the cruise, we edited the continuous OBS data with length of 70 sec and SEG-Y format. At the same time, calibration of the OBS clock for GPS time was carried out using difference times between OBS clock and GPS time, which measured just before OBS deployment and just after OBS retrieval.

Table 3: OBS information. Each recorder using DAT or hard disk is shown by each abbreviation of DAT or "HD". The "BTS" and "HIGH" means that makers of the hydrophone sensor are Benthos Inc. and High Tech Inc., respectively.

	Deployment				Retrieval					
	Time	Coordinate			Time	Coordinate			HD	hyd
Site	UTC	Lat(N)	Lon(E)	Dep (m)	UTC	Lat(N)	Lon(E)	Dep (m)	type	maker
1	7.8 4:56	35°10.8644'	139°11.5669'	762	7.15 21:19	35°10.8218'	139°11.6408'	782	DAT	HIGH
2	7.8 5:28	35°08.2094'	139°12.1667'	457	7.15 22:12	35°08.1680'	139°12.1721'	460	DAT	HIGH
3	7.8 5:55	35°05.5484'	139°12.7808'	576	7.15 23:23	35°05.5072'	139°12.7509'	570	DAT	HIGH
4	7.8 6:20	35°02.9118'	139°13.3604'	670	7.16 0:00	35°02.9106'	139°13.4423'	703	HD	HIGH
5	7.8 6:48	35°00.2519'	139°13.9362'	1263	7.16 1:34	35°00.2297'	139°13.9800'	1270	HD	HIGH
6	7.8 7:27	34°57.5945'	139°14.5231'	1298	7.16 2:39	34°57.5232'	139°14.4469'	1290	DAT	HIGH
7	7.8 8:02	34°54.9467'	139°15.1603'	1256	7.16 4:00	34°55.1402'	139°15.2856'	1274	HD	BTS
8	7.8 9:40	34°44.2570'	139°17.4514'	297	7.16 5:51	34°44.4683'	139°17.6491'	325	HD	HIGH
9	7.8 10:12	34°41.6558'	139°18.0901'	145	7.16 6:51	34°41.7152'	139°18.4259'	140	DAT	HIGH
10	7.8 10:43	34°39.0137'	139°18.5958'	333	7.16 7:43	34°39.0376'	139°19.0497'	319	DAT	HIGH
11	7.8 11:13	34°36.3573'	139°19.1812'	306	7.16 8:38	34°36.4496'	139°19.4808'	316	DAT	HIGH
12	7.8 11:41	34°33.7089'	139°19.7901'	255	7.16 9:26	34°33.7741'	139°19.9467'	259	DAT	HIGH
13	7.8 12:12	34°31.0507'	139°20.4428'	301	7.16 10:18	34°31.2592'	139°20.6534'	297	DAT	BTS
14	7.8 12:45	34°28.3876'	139°20.9857'	248	7.16 11:14	34°28.4215'	139°21.0912'	251	DAT	HIGH
15	7.8 13:17	34°25.6855'	139°21.6055'	106	7.16 12:06	34°25.7198'	139°21.7904'	110	HD	HIGH
16	7.8 13:47	34°23.0837'	139°22.2356'	208	7.16 13:03	34°23.2706'	139°22.5440'	237	DAT	HIGH
17	7.8 14:19	34°20.4285'	139°22.8091'	394	7.16 14:09	34°20.5849'	139°22.8506'	400	DAT	HIGH
18	7.8 14:49	34°17.7792'	139°23.3800'	382	7.16 15:05	34°17.7701'	139°23.2575'	381	DAT	HIGH
19	7.8 15:23	34°15.1387'	139°23.9881'	389	7.16 16:00	34°15.0677'	139°23.8786'	393	HD	BTS
20	7.8 15:56	34°12.4668'	139°24.5943'	451	7.16 16:54	34°12.4592'	139°24.7723'	457	DAT	HIGH
21	7.11 22:58	34°09.8507'	139°25.0148'	378	7.16 18:07	34°09.3949'	139°25.7881'	285	HD	HIGH
22	7.8 16:51	34°07.2018'	139°25.6803'	314	7.16 19:42	34°07.1387'	139°25.7367'	318	HD	HIGH
23	7.8 17:20	34°04.5009'	139°26.0504'	285	7.16 20:33	34°04.5006'	139°26.0446'	292	HD	HIGH
24	7.8 17:45	34°01.9004'	139°26.8982'	388	7.15 9:51	34°01.9816'	139°27.0845'	378	DAT	HIGH
25	7.8 18:15	33°59.2419'	139°27.4990'	511	7.15 8:55	33°59.2952'	139°27.7731'	492	HD	HIGH
26	7.8 18:58	33°56.5311'	139°27.9411'	1028	7.15 7:56	33°56.5760'	139°28.2596'	995	HD	HIGH
27	7.8 19:32	33°53.9034'	139°28.5313'	1240	7.15 6:48	33°53.8957'	139°28.6903'	1250	DAT	HIGH
28	7.8 20:04	33°51.2589'	139°29.1191'	1401	7.27 7:04	33°51.2887'	139°29.2727'	1410	DAT	HIGH
29	7.8 20:34	33°48.6016'	139°29.7104'	1603	7.27 5:47	33°48.4937'	139°30.0545'	1617	HD	HIGH
30	7.8 21:04	33°45.8860'	139°30.3281'	1669	7.27 4:18	33°45.9173'	139°30.6077'	1675	HD	BTS
31	7.8 21:34	33°43.2949'	139°30.8859'	1656	7.27 3:01	33°43.3217'	139°31.0977'	1661	HD	BTS
32	7.8 22:07	33°40.6062'	139°31.4765'	1641	7.27 1:44	33°40.6447'	139°31.7900'	1642	HD	HIGH
33	7.8 22:39	33°37.9795'	139°32.0204'	1631	7.27 0:28	33°38.1335'	139°32.4997'	1629	HD	HIGH
34	7.8 23:10	33°35.2997'	139°32.6232'	1610	7.26 23:14	33°35.5310'	139°33.2396'	1611	HD	BTS
35	7.8 23:41	33°32.6349'	139°33.1111'	1635	7.26 22:04	33°32.9126'	139°33.8683'	1462	DAT	HIGH
36	7.9 0:12	33°29.9827'	139°33.7284'	1312	7.26 20:45	33°30.3000'	139°34.3128'	1375	HD	BTS
37	7.9 0:47	33°27.2991'	139°34.3659'	1109	7.26 19:33	33°27.4036'	139°34.8214'	1087	HD	HIGH
38	7.9 1:22	33°24.6798'	139°34.9178'	355	7.26 18:20	33°24.7132'	139°35.2047'	456	HD	HIGH
39	7.9 2:09	33°22.0034'	139°35.5049'	205	7.26 17:31	33°22.0073'	139°35.6383'	199	HD	HIGH
40	7.9 2:42	33°19.3701'	139°36.0658'	199	7.26 16:47	33°19.4103'	139°36.1891'	215	DAT	HIGH
41	7.9 3:17	33°16.7327'	139°36.6452'	450	7.26 15:59	33°16.7371'	139°36.7787'	455	HD	HIGH
42	7.9 3:56	33°14.0869'	139°37.1988'	792	7.26 15:09	33°14.6081'	139°37.2967'	788	DAT	HIGH
43	7.9 4:30	33°11.4384'	139°37.7551'	855	7.26 14:14	33°11.4838'	139°37.8104'	856	HD	HIGH
44	7.9 5:05	33°08.7407'	139°38.1896'	506	7.26 13:20	33°08.7967'	139°38.2210'	515	DAT	HIGH
45	7.9 5:35	33°06.1083'	139°38.8406'	413	7.26 12:32	33°06.1814'	139°38.7699'	421	HD	HIGH
46	7.9 6:03	33°03.3890'	139°39.5133'	552	7.26 11:51	33°03.5681'	139°39.4259'	600	HD	HIGH
47	7.9 6:31	33°00.8181'	139°40.1269'	564	7.26 11:02	33°00.9204'	139°40.1344'	553	HD	HIGH
48	7.9 6:56	32°58.1394'	139°40.6825'	459	7.26 10:09	32°58.1757'	139°40.7186'	460	DAT	HIGH
49	7.9 7:23	32°55.5031'	139°41.2187'	464	7.26 9:17	32°55.5063'	139°41.2256'	466	DAT	BTS
50	7.9 7:51	32°52.8479'	139°41.8167'	488	7.26 8:22	32°52.8576'	139°41.8712'	495	DAT	HIGH
51	7.9 8:19	32°50.1914'	139°42.3731'	492	7.26 7:30	32°50.1916'	139°42.4449'	498	HD	BTS
52	7.9 8:48	32°47.5329'	139°42.9557'	486	7.26 6:33	32°47.5342'	139°42.9881'	491	DAT	HIGH
53	7.9 9:14	32°44.9051'	139°43.4758'	456	7.26 5:44	32°44.9238'	139°43.4645'	464	HD	BTS
54	7.9 9:40	32°42.2446'	139°44.0417'	441	7.26 4:55	32°42.2137'	139°43.9542'	440	HD	HIGH
55	7.9 10:06	32°39.5916'	139°44.6195'	558	7.26 4:03	32°39.5290'	139°44.4857'	547	HD	HIGH
56	7.9 10:32	32°36.9336'	139°45.1628'	886	7.26 3:06	32°36.8652'	139°45.0266'	914	HD	BTS
57	7.9 10:58	32°34.2739'	139°45.7883'	998	7.26 2:02	32°34.2505'	139°45.7067'	1007	HD	HIGH
58	7.9 11:28	32°31.6313'	139°46.4117'	985	7.26 1:02	32°31.5825'	139°46.3564'	989	HD	HIGH
59	7.9 12:02	32°29.0668'	139°47.7877'	679	7.25 23:59	32°28.9835'	139°47.7030'	652	DAT	HIGH
60	7.9 12:36	32°26.6013'	139°49.5222'	512	7.25 23:00	32°26.4984'	139°49.5077'	453	HD	BTS
61	7.17 4:41	32°23.6573'	139°48.0231'	920	7.25 22:02	32°23.5690'	139°48.2449'	999	HD	HIGH
62	7.17 5:11	32°21.0160'	139°48.5324'	1360	7.25 20:52	32°20.9693'	139°48.8367'	1343	HD	HIGH

Table 3: (continued).

Site	Deployment Time UTC	Deployment Lat(N)	Deployment Lon(E)	Deployment Dep (m)	Retrieval Time UTC	Retrieval Lat(N)	Retrieval Lon(E)	Retrieval Dep (m)	HD type	hyd maker
63	7.17 5:40	32°18.3506'	139°49.1881'	1473	7.25 19:40	32°18.3663'	139°49.5359'	1477	HD	BTS
64	7.17 6:09	32°15.6741'	139°49.6407'	1490	7.25 18:25	32°15.7325'	139°49.8993'	1491	DAT	HIGH
65	7.17 6:37	32°13.6029'	139°50.2472'	1507	7.25 17:13	32°13.1428'	139°50.3812'	1511	DAT	HIGH
66	7.17 7:07	32°10.4126'	139°50.8219'	1371	7.25 16:00	32°10.4202'	139°50.8031'	1370	HD	BTS
67	7.17 7:39	32°07.7590'	139°51.3590'	777	7.25 14:45	32°07.7136'	139°51.2569'	871	DAT	HIGH
68	7.17 8:14	32°05.0347'	139°51.9773'	740	7.25 13:41	32°05.0766'	139°51.8554'	761	HD	HIGH
69	7.17 8:48	32°02.3938'	139°52.5741'	1130	7.25 12:47	32°02.3977'	139°52.4155'	1111	DAT	HIGH
70	7.17 9:23	31°59.7375'	139°53.1017'	1203	7.25 11:43	31°59.8145'	139°52.9783'	1206	DAT	HIGH
71	7.17 9:57	31°57.0879'	139°53.6996'	547	7.25 10:36	31°57.1222'	139°53.5391'	554	HD	HIGH
72	7.17 10:31	31°54.2542'	139°53.0792'	571	7.25 9:33	31°54.2410'	139°53.0278'	599	HD	HIGH
73	7.17 11:08	31°51.6931'	139°54.7198'	509	7.25 8:40	31°51.6639'	139°54.6491'	524	DAT	HIGH
74	7.17 11:41	31°49.0870'	139°55.3074'	685	7.25 7:48	31°49.1061'	139°55.3021'	686	HD	HIGH
75	7.17 12:12	31°46.4370'	139°55.8638'	982	7.25 6:50	31°46.4527'	139°55.1694'	956	HD	HIGH
76	7.17 12:54	31°43.8164'	139°56.4298'	1298	7.25 5:48	31°43.8605'	139°56.5399'	1302	DAT	HIGH
77	7.17 13:24	31°41.1461'	139°56.9711'	1312	7.25 4:37	31°41.2242'	139°57.0474'	1316	HD	HIGH
78	7.17 13:57	31°38.4285'	139°57.4973'	1288	7.25 3:26	31°38.5160'	139°57.4633'	1289	HD	HIGH
79	7.17 14:29	31°35.7668'	139°58.0642'	1233	7.25 2:25	31°35.8296'	139°57.9818'	1232	DAT	HIGH
80	7.17 15:00	31°33.1823'	139°58.6134'	1123	7.25 1:22	31°33.2641'	139°58.6127'	1115	DAT	HIGH
81	7.17 15:32	31°30.5132'	139°59.8531'	384	7.25 0:20	31°30.5848'	139°59.0903'	444	HD	HIGH
82	7.17 16:04	31°27.8560'	139°59.6767'	466	7.24 23:33	31°27.9494'	139°59.5912'	462	HD	HIGH
83	7.17 16:38	31°25.2004'	140°00.2412'	605	7.24 22:44	31°25.2481'	140°00.0941'	607	HD	BTS
84	7.17 17:12	31°22.5731'	140°00.7332'	935	7.24 21:50	31°22.5656'	140°00.4859'	918	HD	HIGH
85	7.17 17:47	31°19.8922'	140°01.3412'	981	7.24 20:51	31°19.9772'	140°01.1996'	982	HD	HIGH
86	7.17 18:20	31°17.2481'	140°01.9020'	746	7.24 19:49	31°17.4175'	140°01.8327'	781	HD	BTS
87	7.17 18:56	31°14.5850'	140°02.4534'	515	7.24 18:51	31°14.7776'	140°02.3930'	502	HD	HIGH
88	7.17 19:45	31°11.8840'	140°03.0239'	1036	7.24 17:56	31°12.1258'	140°02.8968'	1019	HD	HIGH
89	7.17 20:20	31°09.2171'	140°03.5222'	1270	7.24 16:54	31°09.4270'	140°03.4101'	1252	HD	HIGH
90	7.17 20:53	31°06.5626'	140°04.1144'	1383	7.24 15:40	31°06.7778'	140°04.0735'	1373	HD	HIGH
91	7.17 21:23	31°01.9196'	140°04.6504'	1453	7.24 14:33	31°04.1247'	140°04.6286'	1447	HD	HIGH
92	7.17 21:53	31°01.2719'	140°05.1062'	1506	7.24 13:24	31°01.4220'	140°05.1315'	1499	DAT	HIGH
93	7.17 22:24	30°58.6112'	140°05.6668'	1594	7.24 12:14	30°58.7885'	140°05.6968'	1579	HD	HIGH
94	7.17 22:58	30°55.9322'	140°06.2266'	1631	7.24 11:05	30°56.1104'	140°06.2660'	1629	DAT	HIGH
95	7.17 23:32	30°53.2696'	140°06.7287'	1611	7.24 9:50	30°53.3763'	140°06.8534'	1610	HD	HIGH
96	7.18 0:06	30°50.6045'	140°07.2597'	1610	7.24 8:38	30°50.7606'	140°07.4818'	1613	DAT	HIGH
97	7.18 0:38	30°47.9458'	140°07.7964'	1625	7.24 7:25	30°48.1156'	140°08.0447'	1624	DAT	HIGH
98	7.18 1:10	30°45.2803'	140°08.3288'	1616	7.24 6:13	30°40.5523'	140°08.6671'	1620	HD	HIGH
99	7.18 1:42	30°42.6457'	140°08.8618'	1547	7.24 4:57	30°42.8620'	140°09.0339'	1526	HD	HIGH
100	7.18 2:13	30°39.9617'	140°09.4246'	1543	7.24 3:34	30°40.1191'	140°09.6578'	1536	HD	HIGH
101	7.18 2:44	30°37.3478'	140°09.9888'	1524	7.24 2:22	30°37.5083'	140°10.2124'	1516	HD	BTS
102	7.18 3:16	30°34.7220'	140°10.5903'	1321	7.24 1:14	30°34.9411'	140°10.7383'	1342	HD	HIGH
103	7.18 3:46	30°32.0630'	140°11.1398'	1212	7.23 23:53	30°32.2720'	140°11.2453'	1183	DAT	HIGH

Table 4: Sensitivities of geophone and hydrophone sensors.

Sensor type	Sensor name	Maker	Sensitivity	Frequency
Geophone (three components)	L-28LB.H.V	Mark Products	0.69 V/in/sec	4.5Hz (natural freq.)
Hydrophone	AQ-18	Benthos, inc.	-169 dB	1Hz - 12kHz
Hydrophone	HTI-99DY	HIGH TECH, inc	-165dB	2Hz - 20kHz

2.3 Multichannel hydrophone streamer

During airgun shooting, we towed a 12-channel hydrophone streamer to investigate the shallow structures, in particular, a distribution of sediments with low P-wave velocity (Figure 4). The hydrophone streamer (STEALTHARRAY ST-48) cable is solid type made by Input/Output Inc. The interval of each channel was 25 m. The lengths of active section and read-in cable from the stern are 300 m and 150 m, respectively. Hydrophone sensors (TYPE Bruel & Kjaer Free-field 1/2 Microphone) with sensitivity of -25.9dB re1V/Pa (50.4mV/Pa) were used and analog signals from five sensors in the same channel were stacked before A/D conversion. The A/D conversion kit was attached in the

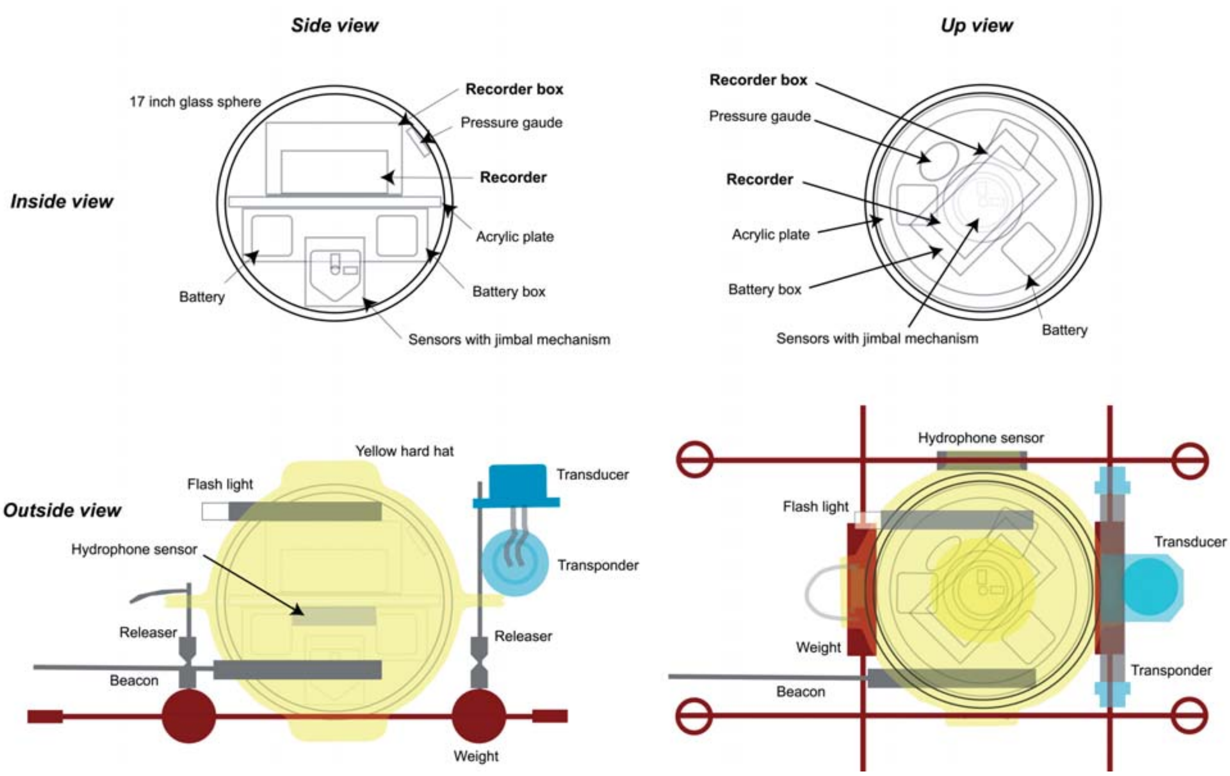

Figure 5: Sketch of our OBS.

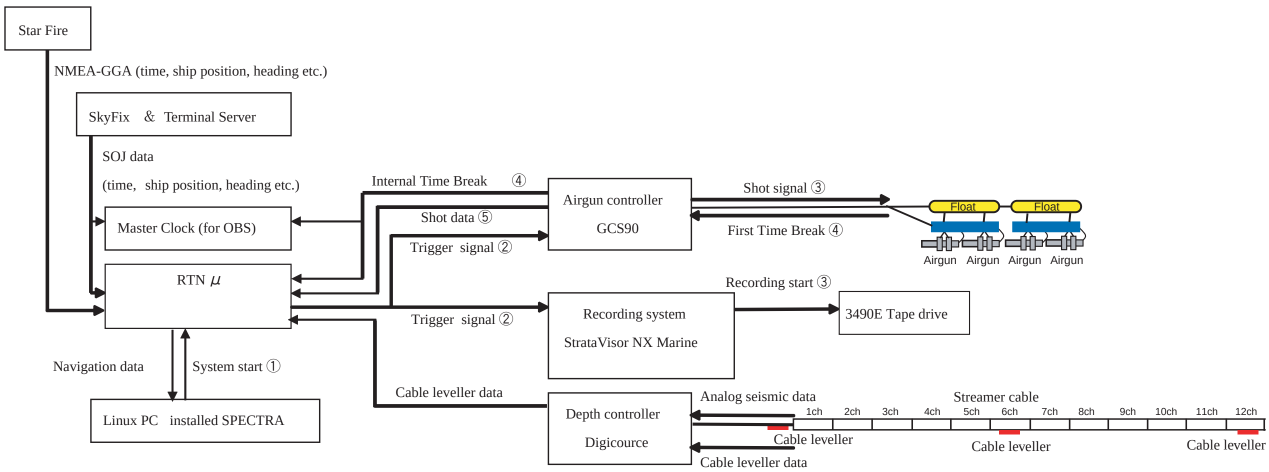

Figure 6: Flow chart for the MCS recording system. Circled numerals show the timing flow of this seismic system.

recording system, the StrataVisor NX Marine made by Geometrics Inc, and digitized data was recorded on 3490E tapes with SEG-D format. No recording delay was set. The sampling rate was 4 msec and the record length was 13.5 sec. Because seismic record from eighth channel is no good during this cruise, we omitted the traces.

2.4 Seismic recording/shooting system

A seismic system of R/V 'Kaiyo' consists of a navigation system with software SPECTRA, a recording system (StrataVisor NX Marine) and a gun controller system (GCS90), and these systems are connected via RTNμ in shown by Figure 6. As mentioned above, we adapted Starfire as a navigation source of seismics. Navigation data collected from Starfire and Skyfix for the ship's navigation system was sent to the RTNμ via the terminal server connected to the ship LAN of the ship and this MCS system. The RTNμ obtains time signals of GPS (Starfire) from original antenna. Then, the navigation data is sent to the PC Linux machine installed SPECTRA software and monitored on the dis-

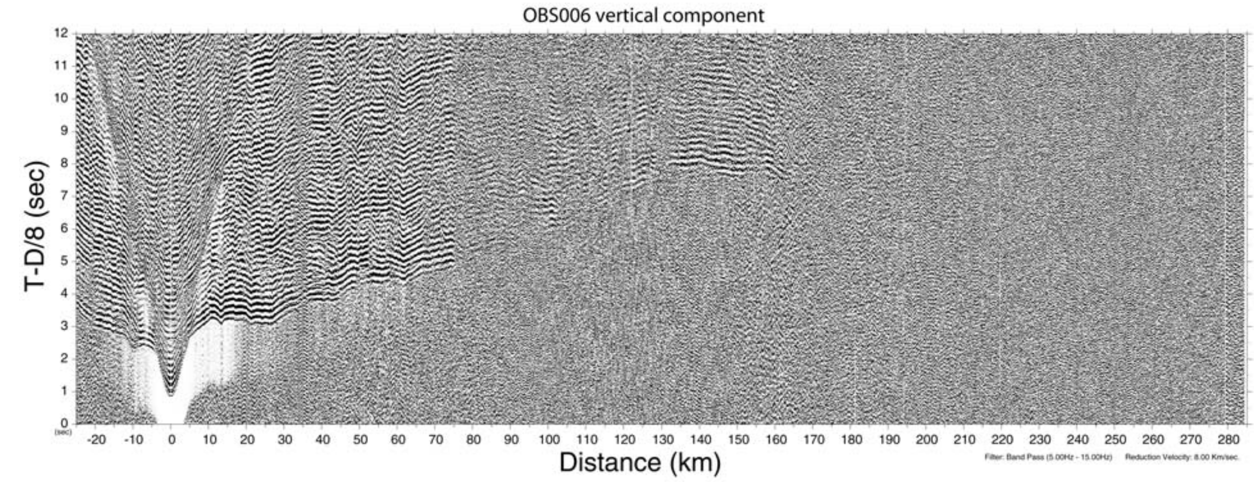

Figure 7: Vertical record section recorded by OBS#6. All traces are filtered by 5-15 Hz. Vertical and horizontal axes are offsets from OBS and reduced traveltimes by 8 km/s.

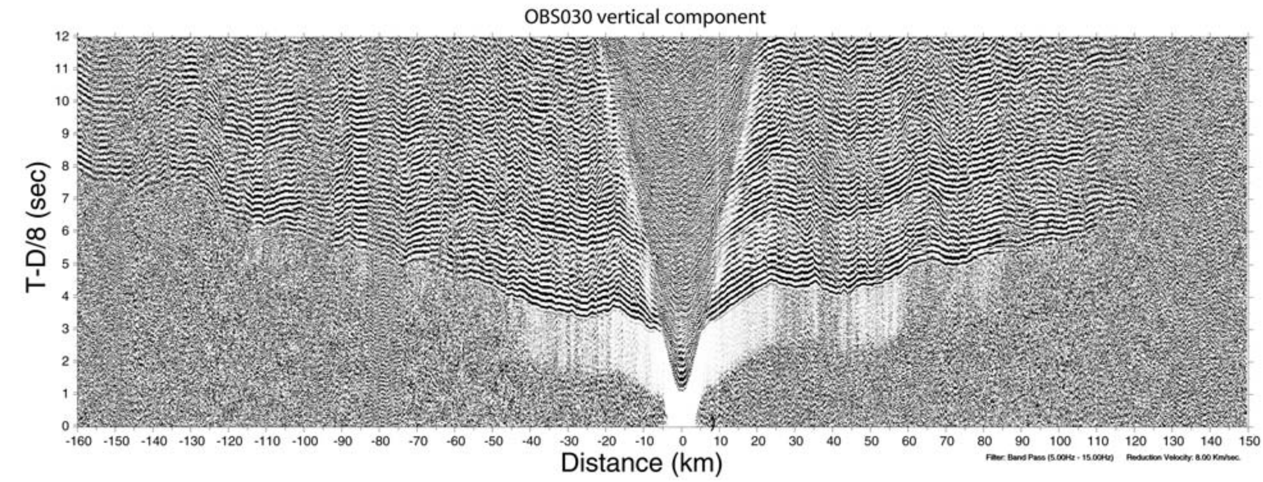

Figure 8: Vertical record section recorded by OBS#30. The details are same as for Figure 7.

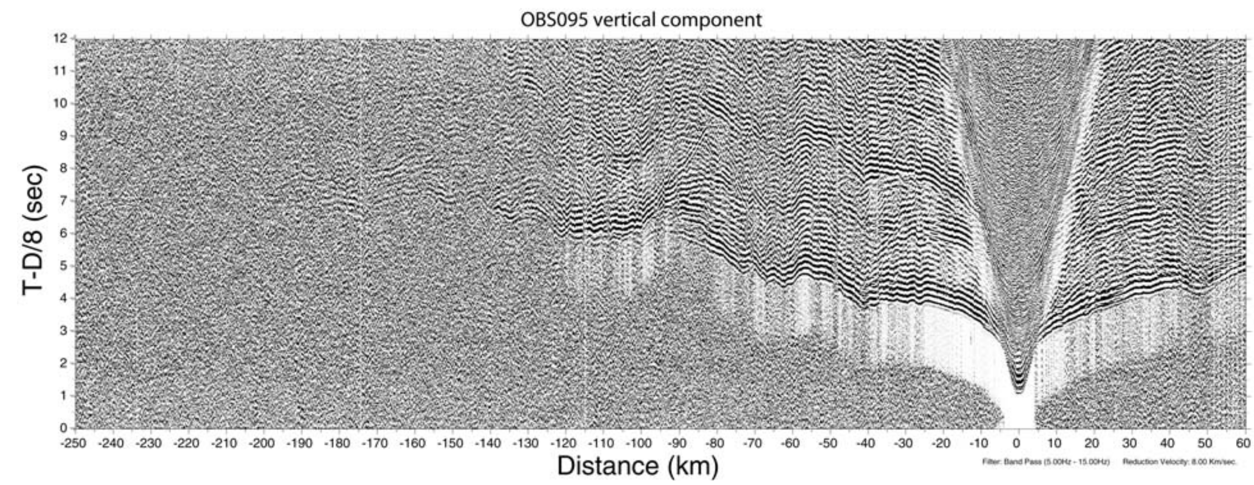

Figure 9: Vertical record section recorded by OBS#95. The details are same as for Figure 7.

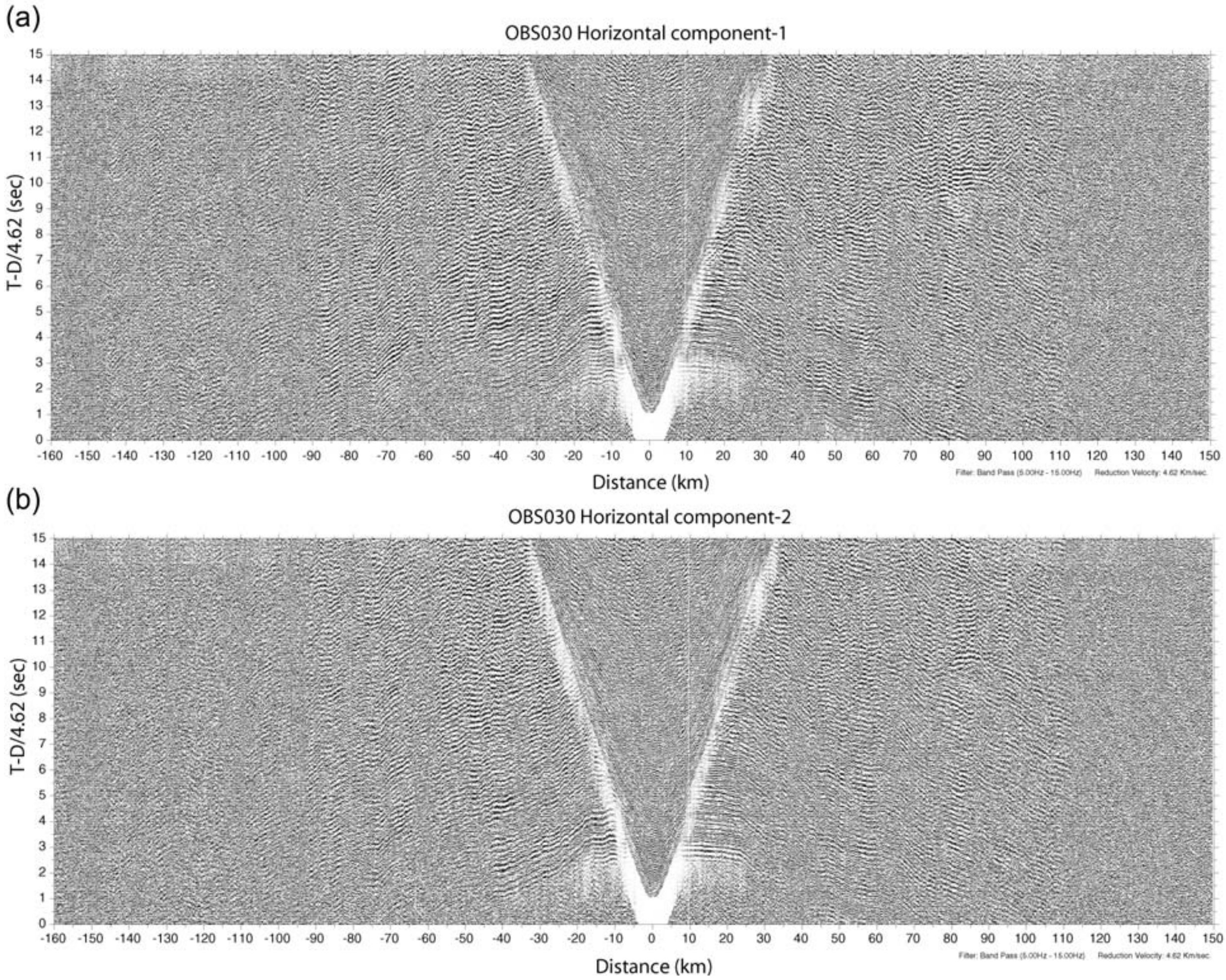

Figure 10: Horizontal record sections recorded by OBS#30. All traces are filtered by 5-15 Hz. The reduced velocity is 4.62 km/s. (a) Horizontal component-1. (b) Horizontal component-2.

play. Timing of the system start, shot number and so on are set on the SPECTRA software. The system start signal generated from the SPECTRA was sent to the gun controller and the recording system as a trigger signal via the RTNμ. The gun controller sends back the internal time break signal to the master clock and RTNμ just after getting trigger signals. Then the trigger signals is sent to eight airguns as shot signals, and the recording system starts to record seismic data from a hydrophone streamer. The first break signal is sent to the gun controller from the airguns at the same timing with the shot, and then the gun controller sends the shot data to RTNμ.

3. Data

In this chapter, we introduce some representative examples of the seismic data obtained by OBSs and MCS. Vertical components of OBS#6, OBS#30 and OBS#95, and horizontal components of OBS#30 are described in section 3.1. MCS data are described in section 3.2.

3.1 OBS

We retrieved all OBSs, however, recording system of five OBSs had troubles. The reason is due to troubles of a sub-standard hard disk or digital audio tape inside the recorder. Except some OBS data with recorder troubles, the data quality of available OBSs is basically good and we can trace the first phases on vertical records until 100 km distance from each OBS. Horizontal records also show good quality despite of poorer S/N ratio than the vertical, and we can see converted S arrivals until about 100 km from the OBS. We describe characteristics of OBS data using vertical record sections of OBS#6 (Figure 7) , OBS#30 (Figure 8) and OBS#95 (Figure 9) as follows.

OBS#6 was deployed in the Sagami Bay. We can trace first arrivals to an offset of 170 km from the OBS (Figure 7). The apparent velocities of the first phases in the northern side are 3.7 km/s, 5.5 km/s and 6.1 km/s for offsets of 3-5 km, 5-10 km and 10-20 km, respectively. In the southern side, we can trace these phases with

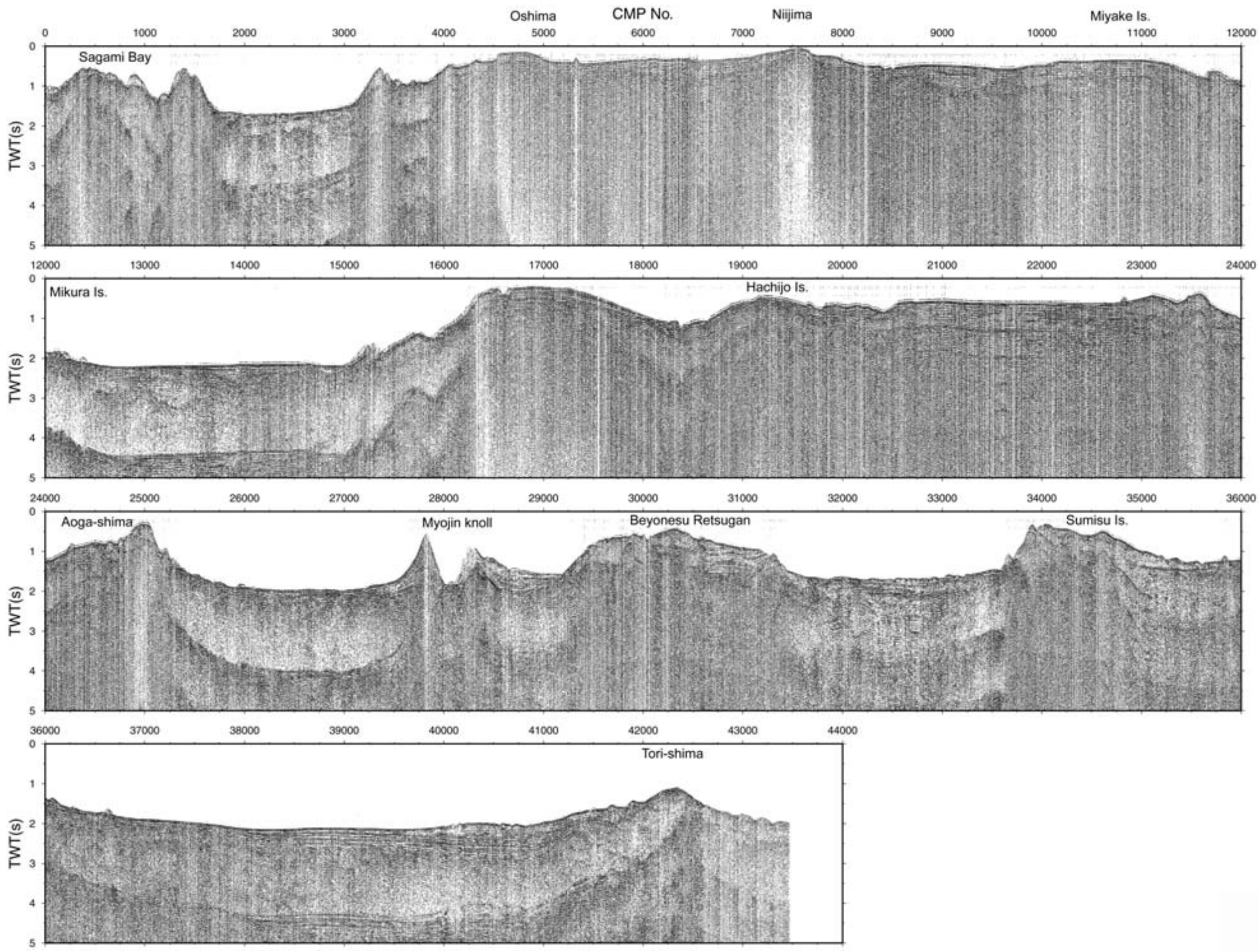

Figure 11: MCS profiles.

apparent velocities of 4.7 km/s, 5.2 km/s, 6.7 km/s and 8.1 km/s to offsets of 11 km, 36 km, 145 km and 160 km, respectively. Variation of these apparent velocities drawing concave shape can be seen at offsets of -10 km, 20-30 km and 60-65 km due to some volcanoes. Reflections from the Moho (PmP) with high amplitudes can be also seen at an offset of 120-160 km.

OBS#30 was deployed on the southwestern offshore of Mikura Island. On the northern side, we can trace first phases with apparent velocities of 3.9 km/s, 5.0 km/s, 6.0 km/s, 6.5 km/s and 7.2 km/s in offsets of 5-6 km, 6-30 km, 30-50 km, 50-122 km and 150-155 km, respectively. In southern side, the apparent velocities of these phases are 3.9 km/s, 5.0 km/s and 6.9 km/s for offsets of 5-8 km, 8-24 km and 80-105 km, respectively. We can see the apparent velocity variation of first phases in the offsets of 30-80 km. This variation seems to be originated from the topography near the Hachijo Island and the Aoga-shima. Reflections from the Moho (PmP) with high amplitudes can be seen also at the northern offset of 100-120 km and the southern offset of 90-130 km.

OBS#95 was deployed between Sumisu Island and Tori-shima. We can trace the first phases with apparent velocities of 3.9 km/s, 5.2 km/s, 6.2 km/s and 7.4 km/s in offsets of 4-7 km, 7-16 km, 16-25 km and 30-36 km, respectively. Two concave peaks of the variation of these phases were observed, which corresponds to the Sumisu Island and the Beyonesu Retsugan, respectively. In the southern part, the apparent velocity of the first phases are 4.5 km/s, 5.5 km/s, 6.1 km/s and 7.6 km/s in offsets of 4-10 km, 10-20 km, 20-38 km and 38-41 km, respectively. These variation is also effected the topography near the Tori-shima.

These record sections suggest roughly that the crustal structure of the northern part is thicker than that of the southern part according to the offsets identified refractions with apparent velocity of 6.5-7.5 km/s. On the record section of OBS#30, the offset identified the PmP phases with high amplitude is nearer in the southern side. This characteristic suggests also that the northern arc has thick crust than the southern part.

Figures 10a and 10b indicate two horizontal components of OBS#30 crossing perpendicular with each other. We can see many phases with the same apparent

P-wave velocities. This record section seems to have much PSP phases. At the offset of 40-90 km and 8-11 sec in reduced time by 4.62 km/s in southern side, we can see some phases with slow apparent velocities and these phases correspond probably to PSS phases.

3.2 MCS

The reflection data recorded by 12-channel hydrophone streamer has also enough quality to pick the acoustic basement (Figure 11). Applied flows were a collection of spherical divergence, editing bad quality traces, a time variant filter (3-125 Hz), sorting by CDPs, an NMO correction with water velocity of 1500 m/s, a predictive deconvolution filtering using an operator length of 300 ms and an predictions distance of 24 ms, stacking, a time variant bandpass filter of 20-50 Hz and the auto gain control. Because of the channel interval of 25m and the shot interval of 200 m, the fold number was 1 or 2.

We interpret the shallow structure from rough characteristics of reflection image. Thick sediments under concave topography between the Sagami Bay and the Oshima, a small seamount with the intrusion at the northern offshore of the Oshima, thick sediments again under a flat seafloor between the Miyake and the Hachijo Islands can be seen. We can identify sediments between the Aoga-shima and the Myojin knoll, a caldera of the Myojin knoll with a height of about 1,200 m and thick sediments between the Sumisu Island and Tori-shima. At this moment, we cannot identify any proofs of crustal shortening between the Oshima and the Miyake Island relating to the new subduction at southern foot of the Zenisu ridge from this reflection image. After we process reflection data more or we get new reflection data using a 204-channel hydrophone streamer, we will try to identify such proofs showing the crustal deformation.

4. Summary

Due to good data quality of the OBSs, we can trace the first P-arrivals to the offsets of 100 km from each OBS. These OBS record sections suggest that the northern part of the Izu-Ogasawara arc has thicker crust than the southern part. The reflection image indicates the strong heterogeneity for the shallow structure. We will estimate the velocity structural variation over the entire of the arc-arc collision zone and general oceanic arc, and believe that we can clarify the crustal deformation by the collision.

Acknowledgement

We greatly appreciate to following members of KY0408 cruise shipboard party described following, and would not be able to get succession of this seismic experiment without their efforts. We thank Dr. T. Tsuru, Dr. S. Miura, Dr. A. Nakanishi and Dr. J-O Park for planning discussion of this cruise. Moreover, we acknowledge Dr. Wonn Soh giving administrative helps to us.

Marine technicians

Chief Technician	Makoto Ito
Technician	Hitoshi Tanaka
Technician	Masato Sugano
Technician	Yuki Ohwatari
Technician	Morifumi Takaesu
Technician	Nobuo Kojima
Technician	Maiko Kimino
Technician	Hiroyoshi Shimizu
Technician	Michiaki Kudoh
Technician	Kimiko Serizawa
Technician	Yoko Okamoto
Technician	Yusuke Ono
Technician	Yuko Yokozawa (leg1 only)
Technician	Kozue Kurihara (leg1 only)

Crew

Captain	Hitoshi Tanaka
Chief Officer	Hiroaki Masujima
Second Officer	Takamichi Inoue
Third Officer	Toshiyo Ohara
Third Officer	Kenta Oya
Chief Engineer	Tatsuo Jidozono
First Engineer	Akimitsu Fukuda
Second Engineer	Takeshi Settai
Third Engineer	Fumihiko Natsui
Chief Radio Officer	Tokinori Nasu
Second Radio Officer	Katsutoshi Kitamura
Third Radio Officer	Yusuke Takeuchi
Boatswein	Shoichi Abe
Able seaman	Kinya Shoji
Able seaman	Syuichi Yamamoto
Able seaman	Kaname Hirozaki
Able seaman	Yuki Yoshino
Able seaman	Yutaka Sato
Able seaman	Yudai Tayama
No.1 Oiler	Kiyoshi Yahata
Oiler	Hiroyuki Sato
Oiler	Tsuneo Harimoto
Oiler	Keigo Kawai
Assistant Oiler	Shota Watanabe
Chief Steward	Takeshi Miyauchi
Steward	Toshiharu Kishita
Steward	Jihei Nakatsuka

Steward Kazunori Nagano
Steward Takahiro Abe

Reference

1) Aoike, K., W. Soh, H. Tokuyama and A. Taira, Tectonics of Izu collision zone and the crustal materials circulation, *Monthly Chikyu*, extra. No. **32**, 181-190 (2001).
2) Kanazawa,T and H. Shiobara, Newly developed ocean bottom seismometer, Prog. Abst. Japan Earth and Planetary Science Meeting, **2**, 240 (1994).
3) Karig, D. E. and G. F. Moore, Tectonic complexities in the Bonin arc system, *Tectonophysics*, **27**, 97-118 (1975).
4) Macpherson, C. G. and R. Hall, Tectonic setting of Eocene boninite magmatism in the Izu-Bonin-Mariana forearc, *Earth Planet. Sci. Lett.*, **186**, 215-230 (2001).
5) Nakanishi, A., H. Shiobara, R. Hino, S. Kodaira, T. Kanazawa and H. Shimamura, Detailed subduction structure across the eastern Nankai trough obtained from ocean bottom seismographic profiles, *J. Geophys. Res.*, **103**, 27151-27168 (1998).
6) Nishizawa, A., K. Kaneda, H. Seta, K. Terai, T. Yoshida, O. Yokoo, S. Tani, A. Nakanishi, S. Kodaira, N. Takahashi, W. Soh, Y. Kaneda and K. Suyehiro, Crustal structure across the mid Izu-Ogasawara Island arc, *Monthly Chikyu*, extra. No. **43**, 143-151 (2003).
7) Okino, K., S. Kasuga and Y. Ohara, A new scenario of he Parace Vela basin genesis, *Mar. Geophys. Res*., **20**, 21-40 (1998).
8) Shinohara, M., K. Suyehiro, S. Matsuda and K. Ozawa, Digital recording ocean bottom seismometer using portable digital audio tape recorder. *J. Jpn. Soc. Mar. Surv. Tech.*, **5**, 21-31 (1993). (Japanese with English abstract)
9) Shiobara, H. A. Nakanishi, S. Kodaira, R. Hino, T. Kanazawa, H. Shimamura, Seismicity and crustal structure around the eastern Nankai Trough by ocean bottom seismograpic observation, EOS Trans., AGU, Fall meeting, F704 (1996).
10) Suyehiro, K., N. Takahashi, Y. Ariie, Y. Yokoi, R. Hino, M. Shinohara, T. Kanazawa, N. Hirata, H. Tokuyama, and A. Taira, Continental crust, crustal underplating, and low-Q upper mantle beneath an oceanic island arc, *Science*, **272**, 390-392 (1996).
11) Taira, A., S. Kiyokawa, K. Aoike, and S. Saito, Accretion tectonics of the Japanese islands and evolution of continental crust. C.R. Acad. Sci. Paris, Sceinces de la terre et des planetes, **325**, 467-478 (1997).
12) Takahashi, N., K. Suyehiro and M. Shinohara, Implications from the seismic crustal structure of the northern Izu-Ogasawara arc, *Island arc*, **7**, 383-394 (1998).
13) Takahashi, N. H. Amano, K. Hirata, H. Kinoshita, S. Lallemant, H. Tokuyama, F. Yamamoto, A. Taira and K. Suyehiro, Faults configuration around the eastern Nankai trough deduced by multichannel seismic profiling, *Marine Geology*, **187**, 31-46 (2002)
14) Tamura, Y. Y. Tatsumi, D. Zhao, Y. Kido and H. Shukuno, Hot fingers in the mantle wedge; new insights into magma genesis in subduction zones, *Earth Planet. Sci. Lett.*, **197**, 105-116 (2002)
15) Tatsumi, Y., "A review considers the processes involved in the ocean subduction zone as a zero-emission factory, a Subfac, which include ocean plate caving-in (conveyor) to input mantle wedge materials (raw material), volcanoes (stack emissions), and magma (products) without waste emission", Kagaku, **72**, 1154-1157 (2002). (in Japanese)
16) Tatsumi Y. amd Project IBM Core Members, Project IBM: towards a comprehensive understanding of arc evolution and continental crust formation, Abstracts, 111st Ann. Meeting, Geol. Soc. Japan, O-46 (2004).

(Received December 22, 2004)